

## Improved Resistive Switching Uniformity of a Bilayer TiO<sub>2</sub> Films

Insung Kim<sup>1</sup>, Seungjae Jung<sup>1</sup>, Jungho Shin<sup>1</sup>, K.P. Biju<sup>1</sup>, Kyungah Seo<sup>2</sup>, Manzar siddik<sup>1</sup>,  
X.J. Liu<sup>1</sup>, Jaemin kong<sup>1,3</sup>, KwnagheeLee<sup>1,2,3</sup>, and Hyunsang Hwang<sup>1,2</sup>

Department of Materials Science and Engineering<sup>1</sup>,  
Department of Nanobio Materials and Electronics<sup>2</sup>,

Heeger Center for Advanced Materials<sup>3</sup>, Gwangju Institute of Science and Technology

261 Cheomdan-gwagiro (Oryong-dong), Buk-gu, Gwangju 500-712, Republic of Korea

Phone: +82-62-715-2314, Fax: +82-62-715-2304, e-mail: hwanghs@gist.ac.kr

### 1. Introduction

We investigated the resistive switching properties of bilayer TiO<sub>2</sub> thin films using 250nm via-hole structure. Sol-gel method has various advantages such as low cost, simplified manufacturing and large area applications. However, compared with conventional deposition process, films deposited by sol-gel method show inferior electrical characteristics and uniformity for nano-scale device applications.

In this study, to solve the problems of conventional sol-gel device, we have investigated the effects of additional atomic layer deposition (ALD) TiO<sub>2</sub> (~8 nm) layer on resistive switching behavior.

### 2. Experimentals

Pt/TiO<sub>2-x</sub>/TiO<sub>2</sub>/W device were fabricated using 250 nm via-hole substrate as shown in Fig. 1(a). After depositing 8nm-thick TiO<sub>2</sub> layer by ALD (defined here as TiO<sub>2</sub>), 50nm-thick sol-gel layer (defined here as TiO<sub>2-x</sub>) was prepared by spin coating. TiO<sub>2</sub> solution made of Titanium (IV) isopropoxide according to the previous work reported elsewhere [1]. The resulting films were thermally annealed at 400°C for 2h under a nitrogen atmosphere. Using the cross-sectional transmission electron microscopy (TEM) images as shown in Fig (b), we have confirmed a Pt/TiO<sub>2-x</sub>/TiO<sub>2</sub>/W structure. Crystalline TiO<sub>2</sub> layer can also be confirmed from the TEM figure. After conventional lithography process, a 100nm-thick Pt top electrode was deposited by sputtering.

### 3. Result& Discussion

To confirm the concentration of oxygen in each layer, X-ray photoelectron spectroscopy (XPS) analysis was performed as shown in Fig. 2. The Ti 2p<sub>1/2</sub> and 2p<sub>3/2</sub> XPS peaks were resolved into two spin-orbits, which were assigned to Ti<sup>3+</sup> and Ti<sup>4+</sup> peak [2]. Because the Ti 2p area ratio of the Ti<sup>3+</sup> to the Ti<sup>4+</sup> peak can show the defect concentration of Ti<sup>3+</sup>, we calculated defect ratio for TiO<sub>2</sub> and TiO<sub>2-x</sub> layer results 0.17 and 0.23 respectively [3]. This indicates that the TiO<sub>2-x</sub> layer has a significant number of oxygen vacancy compared to TiO<sub>2</sub> layer. Fig. 3 (a) shows bipolar switching characteristics of TiO<sub>2-x</sub>/TiO<sub>2</sub> film. After forming process, the devices switch from HRS to LRS by applying positive bias. We can change the resistance state back to HRS by applying negative bias. Inset of Fig. 3(b) shows switching characteristics of Pt/TiO<sub>2-x</sub>/W structure. The switching characteristic of Pt/TiO<sub>2-x</sub>/W device shows more fluctuation than Pt/TiO<sub>2-x</sub>/TiO<sub>2</sub>/W device. Statistical distribution of switching parameters (I<sub>ON</sub> and I<sub>OFF</sub>) for the TiO<sub>2-x</sub>/TiO<sub>2</sub> and TiO<sub>2-x</sub> layer were depicted in Fig. 4 (a). The distribution of 50 cell to cell uniformity in TiO<sub>2-x</sub>/TiO<sub>2</sub> layer shows in Fig.4 (b), and the average value and

standard deviation of I<sub>ON</sub> and I<sub>OFF</sub> are summarized in Table.1. Significant improvement of switching uniformity was observed by adopting TiO<sub>2</sub> layer. Endurance characteristics of the TiO<sub>2-x</sub>/TiO<sub>2</sub> devices were investigated as shown in Fig. 5. We have confirmed that TiO<sub>2-x</sub>/TiO<sub>2</sub> devices exhibit high ON/OFF ratio (>10<sup>2</sup>-10<sup>3</sup>) up to 10<sup>4</sup> cycles. The retention property at room temperature is shown in Fig.6, and there are no significant changes in the resistance magnitudes up to 10<sup>4</sup>sec.

We propose the conduction model for the TiO<sub>2-x</sub>/TiO<sub>2</sub> structure shown in Figure 7. Sol-gel layer is highly conducting film with lots of oxygen vacancies (V<sub>O</sub><sup>2+</sup>) and ALD layer is highly resistive. To confirm the switching mechanism, we measured I-V curve with varying bias windows (2V, 5V, and 7V). As shown in Figure. 7(a), the negatively charged oxygen ions (O<sup>2-</sup>) are attracted and move into TiO<sub>2-x</sub> layer. Such ionic movement towards top electrode reduces the thickness of the insulating TiO<sub>2</sub> region which in turn causes LRS state. In contrast, by applying negative bias as shown in (Fig. 7 (b)), oxygen ions (O<sup>2-</sup>) move back to their original place which in turn causes HRS state [4-5].

### 4. Summary

Improved resistive memory based on solution process was intensively investigated. A resistive memory device with additional TiO<sub>2</sub> layer shows improved switching uniformity that can be explained by exchanging oxygen ion between undoped (TiO<sub>2</sub>) and doped layer (TiO<sub>2-x</sub>). Our approach shows promise for future low-cost, large area flexible memory applications.

### Acknowledgements

This work was supported by the national research program of the 0.1 Terabit Non-volatile Memory Development Project, the National Research Laboratory (NRL) Programs of the Korea Science and Engineering Foundation (KOSEF) and the World Class University (WCU) program at GIST through a grant provided by the Ministry of Education, Science and Technology (MEST) of Korea.

### References

- [1] J. Kim et al., Advanced materials, **18** (2006) 572
- [2] C. Lee et al., Langmuir Letter, **25** (2009) 4274
- [3] S. W et al., Metals and materials international, **14** (2008) 759
- [4] M. J. Kumar., IETE technical review, **26** (2009)
- [5] R. S. Williams., Nature Nanotechnology, **3** (2008) 28

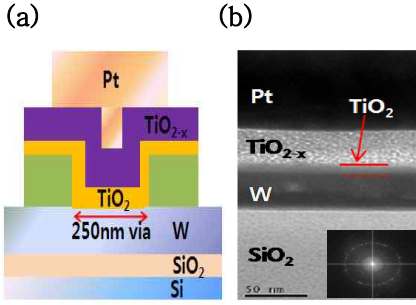


Fig.1 (a) Schematic view of Pt/TiO<sub>2-x</sub>/TiO<sub>2</sub>/W 250nm via-hole structure. (b) Cross-sectional TEM images and diffraction pattern of TiO<sub>2</sub> layer.

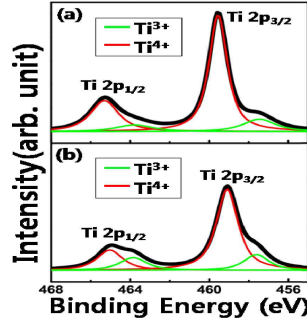


Fig.2 The binding energy of Ti 2p<sub>1/2</sub> and 2p<sub>3/2</sub> were measured by XPS (a) ALD deposited TiO<sub>2</sub> (b) Spin-coated TiO<sub>2-x</sub>

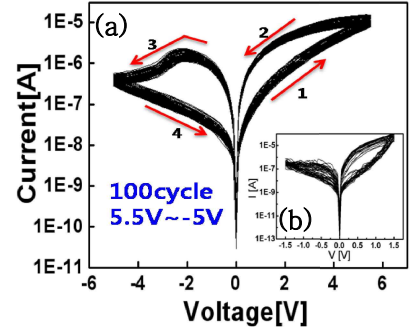


Fig.3 I-V hysteresis of different structure (a) Pt/TiO<sub>2-x</sub>/TiO<sub>2</sub>/W (b) Pt/TiO<sub>2-x</sub>/W

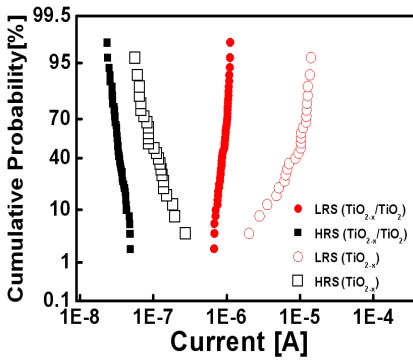
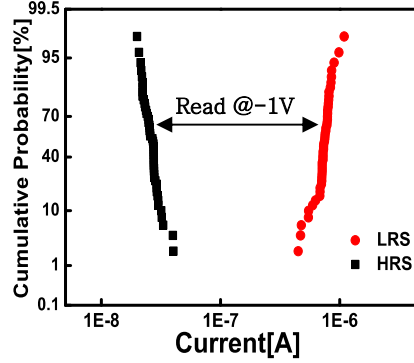


Fig.4 Cumulative probability of current distributions for HRS and LRS (a) One cell uniformity of TiO<sub>2-x</sub>/TiO<sub>2</sub> and TiO<sub>2-x</sub> structure (b) 50 cell to cell uniformity of TiO<sub>2-x</sub>/TiO<sub>2</sub> structure.



(a) One cell uniformity

	AVG of log <sub>10</sub> (I <sub>low</sub> )	AVG of log <sub>10</sub> (I <sub>high</sub> )	①STD of log <sub>10</sub> (I <sub>low</sub> ), ②ΔI/σ	①STD of log <sub>10</sub> (I <sub>high</sub> ), ②ΔI/σ
With ALD (Read@-1V)	-6.04	-7.48	①0.07 ②20.57	①0.08 ②18
W/O ALD (Read@0.7V)	7.00	5.08	①0.18 ②10.7	①0.23 ②8.35

(b) 50 cell to cell uniformity

	AVG of log <sub>10</sub> (I <sub>low</sub> )	AVG of log <sub>10</sub> (I <sub>high</sub> )	①STD of log <sub>10</sub> (I <sub>low</sub> ), ②ΔI/σ	①STD of log <sub>10</sub> (I <sub>high</sub> ), ②ΔI/σ
With ALD (Read@-1V)	-6.13	-7.59	①0.1 ②14.6	①0.09 ②16.22

Table. 1

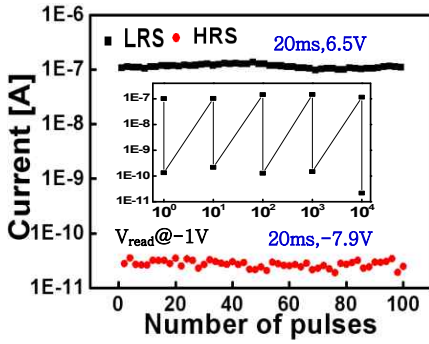


Fig.5 Pulse switching properties of the Pt/TiO<sub>2-x</sub>/TiO<sub>2</sub>/W device for 10<sup>4</sup> cycles.

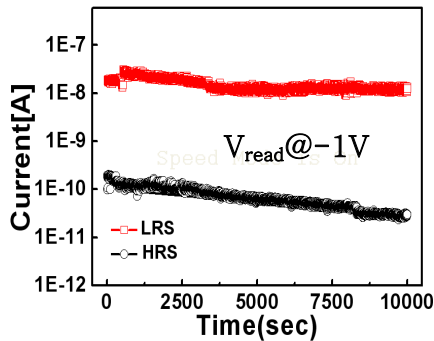


Fig.6 The retention property of the Pt/TiO<sub>2-x</sub>/TiO<sub>2</sub>/W device at room temperature.

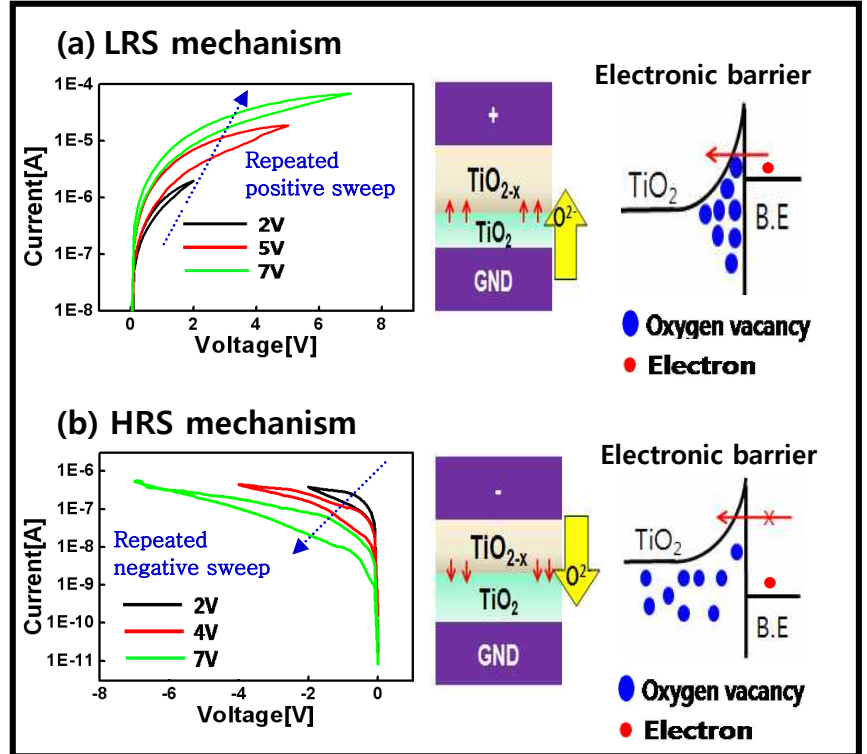


Fig.7 Scheme of the proposed conduction model for the TiO<sub>2-x</sub>/TiO<sub>2</sub> structure. (a), (b) As applied voltage, change insulating layer thickness and schottky barrier between TiO<sub>2</sub> layer and bottom electrode.